scientific reports

Check for updates

OPEN

# Decoding the amniotic membrane transcriptome during equine ascending placentitis

Sophia P. Marchio[1], Hossam El-Sheikh Ali[2], Matthew A. Scott[3], Claudia Barbosa Fernandes[4], Kirsten E. Scoggin[2], Mats Troedsson[2] & Yatta Boakari[1]✉

**Despite its critical role in protecting the fetus, the amniotic membrane remains poorly understood in the context of disease response. The equine amniotic membrane is an important physical barrier to the amniotic compartment, and there is evidence that it may contribute to surfactant synthesis. Surfactants are essential for normal fetal lung development, and disruptions in its availability may be linked to future neonatal complications. Therefore, understanding the molecular changes that occur in fetal-maternal tissues during placentitis would clarify how this condition leads to abortion, preterm delivery, and stillbirth, and identify new strategies to manage the adverse outcomes. Thus, we used RNA sequencing, bioinformatic methods, and immunohistochemistry to characterize the equine amniotic membrane gene expression during experimentally induced ascending placentitis (placentitis group, *n* = 6) compared to gestationally matched control groups (control group, *n* = 6) at 288 days of gestation. We identified 288 differentially expressed genes (DEG) in the placentitis group compared to the control group. Placentitis was associated with the upregulation of toll-like receptors (*TLR4*), prostaglandin synthesis (*PTGS2* and *PTGES*), apoptosis (*MMP9* and *CASP3)*, and hypoxia-associated genes (*SOD2*, *BNIP3*, and *HMOX1*). Our RNA sequencing results were supported by the visual identification of two of those proteins (TLR4 and PTGS2) in the immunohistochemistry analysis. Functional annotation revealed significant enrichment between the DEGs and the toll receptor signaling pathway, which may be a key factor negatively affecting placental functions. In conclusion, our study revealed that the amniotic membrane is not only a physical barrier but also plays an active role in immune response during ascending placentitis.**

**Keywords** Mare, Placentitis, Amnion, *Streptococcus equi* ssp *zooepidemicus*, RNA sequencing

Ascending placentitis affects approximately 1 to 5% of pregnancies in mares[1,2]. This placental infection is responsible for 9.8 to 33.5% of diagnosed abortions, stillbirths, late-term pregnancy losses, and neonatal deaths in the equine industry[1,2]. It is believed to be the result of bacterial migration from the vagina to the cervix, spreading between the uterus and chorioallantois, causing placental separation, myometrial contractility, and, consequently, preterm delivery or abortion[2,3]. The most commonly isolated bacteria in ascending placentitis cases are *Streptococcus equi* ssp. *zooepidemicus*[1,2,4]. Even when the neonate survives, placentitis can still critically compromise the foal's health due to exposure to an inflamed and infected intrauterine environment[3].

The most common diagnostic method currently utilized for placentitis is measuring the combined thickness of the uterus and placenta (CTUP) and assessing placental separation areas through transrectal ultrasound[5]. Measuring steroid hormones[6] and acute-phase proteins such as serum amyloid A[7–9] can complement the diagnosis. However, all current diagnostic methods have limitations. For instance, CTUP measurements may lead to false positives, steroid hormones can vary throughout gestation, and acute-phase proteins are not specific to placentitis[10]. Current treatment protocols aim to decrease uterine contractions and eliminate inflammation and bacterial infection[11]. Although pharmacological strategies have been broadly investigated, their clinical applications, effectiveness, and limitations are not yet fully understood. For example, there are inconsistent therapeutic levels of antibiotics and anti-inflammatories within placental tissues, and limited effectiveness of tocolytics that may even hasten delivery. Additionally, while synthetic progestagens are used, their exact

[1]College of Veterinary Medicine and Biomedical Sciences, Texas A&M University, College Station, TX, USA. [2]Department of Veterinary Science, Maxwell H. Gluck Equine Research Center, University of Kentucky, Lexington, KY, USA. [3]Veterinary Education, Research, and Outreach Center, Texas A&M University, Canyon, TX, USA. [4]Department of Animal Reproduction and Veterinary Radiology, School of Veterinary Medicine and Animal Science, University of São Paulo, São Paulo, SP, Brazil. ✉email: yboakari@cvm.tamu.edu

mechanisms and efficacy in this context remain unproven[12]. Therefore, understanding the molecular and gene-level mechanisms underlying ascending placentitis is of great importance to develop better diagnostic methods and more effective treatments to prevent preterm delivery and abortions.

Ascending placentitis in mares shares similarities with intra-amniotic infection (chorioamnionitis) in women, which is also largely caused by bacterial migration from the vagina and further invasion of the chorioamnion[13]. To better understand the molecular mechanisms involved in intra-amniotic infection, studies have utilized RNA sequencing as a discovery approach to evaluate gene expression in fetal membranes and fetal fluids in humans[14–17]. Investigators identified inflammatory and immunological pathways that were upregulated in human preterm delivery[16]. Elevated expression of heat-shock proteins, such as HSPA5, has been observed to play a role in human spontaneous preterm births, where it appears to promote proinflammatory cytokine expression[18]. Important genes involved in inflammation have also been identified in severe preterm birth in women, including *IL1B*, *TNF*, *IL24*, and *CXCL10*[16]. In mares, similar results have been observed after evaluating RNA sequencing of the chorioallantois membrane from ascending placentitis, characterized by inflammatory and immunological responses, as evidenced by the upregulation of genes encoding key regulators such as toll-like receptors (TLRs), NOD-like receptors (NLRs), and heat-shock proteins (*HSPA6* and *HSPA2*)[19]. However, the overall structure and function of the placenta differ substantially between humans and horses. Humans have a hemochorial placenta, while mares have an epitheliochorial placenta[20,21]. These anatomical differences are important when comparing mechanisms of infection and inflammation between species.

In addition to fetal membranes, other tissues also respond to placentitis in mares[19,22–25]. Upon experimentally induced *Streptococcus equi* ssp. *zooepidemicus* infection, the cervix showed clear signs of remodeling, dominated by inflammatory signaling[23–25]. In the cervix, the overrepresented pathways included toll-like receptor signaling, interleukin signaling, T cell activation, and B cell activation, along with the upregulation of extracellular matrix remodeling-related genes, which were also observed in normal prepartum mares such as *ADAMTS1* and *ADAMTS4*[23]. In the myometrium, activation of contraction-associated genes (*PTGER3*, *PTGS2*, *MMP1*, *MMP8*, and *GJA4*) was observed, triggered by inflammatory and toll-like receptor signaling pathways[22]. This inflammatory response corresponds to changes in the chorioallantois membrane and endometrium that also had overrepresented inflammatory and toll-like receptor signaling pathways[19].

The amniotic membrane is the closest membrane to the fetus, and transcriptomic dysregulations can interfere directly with the amniotic fluid composition and, consequently, with the fetus's health. However, there are no previous reports that identified changes in the amniotic membrane during ascending placentitis in mares. Therefore, the primary aim of this study was to characterize, for the first time, the transcriptomic profile of the amniotic membrane in mares with ascending placentitis compared to those with healthy pregnancies, using RNA sequencing. A secondary aim was to identify biological pathways associated with ascending placentitis through functional annotation analysis. We hypothesize that ascending placentitis will affect the amniotic membrane transcriptome, leading to the upregulation of inflammation-related genes and, consequently, a coordinated immune response across the amniotic membrane.

## Results

### Reproductive parameters

Results of inflammation and placentitis were presented in a previous study[19]. Briefly, placentitis was confirmed by a histopathological analysis of the chorioallantois. Mild to marked inflammation with leukocytic infiltration was identified in the chorioallantois membrane of mares in the placentitis group (Supplementary Table S1). In addition, through transrectal ultrasound examination, a significant ($P < 0.01$) increase in CTUP between the day of inoculation and the day of euthanasia was characterized. Placental separation was present in all mares in the placentitis group, while none was seen in the control group mares. During sample collection, all placentas from the placentitis group were confirmed to have gross lesions consistent with placental infection. However, lesion size was not assessed. Microbiological culture identified *Streptococcus equi* subsp. *zooepidemicus* as the only bacterial isolate in all affected placentas, with no evidence of mixed bacterial growth. All fetuses appeared to be viable at the time of euthanasia.

### Differential gene expression

Based on counts per million, a total of 288 genes were considered differentially expressed (DEG) (P-value < 0.0024) in the amniotic membrane at 288 days of gestation, which is represented in Fig. 1. Within this DEG list (Supplementary Table S2), 177 genes were upregulated and 111 downregulated in the placentitis group compared to the non-placentitis group.

### Comparison of DEGs across other tissues

Comparing the DEGs (FDR < 0.05) across the amniotic membrane, chorioallantois, endometrium, and myometrium, we identified eight genes that were upregulated in all the tissues during ascending placentitis (*AOAH*, *SOD2*, *LOC100053579*, *ITGAX*, *LOC100067491*, *CEBPD*, *IL2RG*, *OAF*) (Supplementary Table S8 and Supplementary Fig. S3). Some genes were only expressed in the amniotic membrane when compared to other tissues, with 42 being upregulated and 43 being downregulated.

### Weighted gene co-expression network construction (WGCNA) and module-trait correlation with placentitis

All filtered genes ($n = 32{,}004$) were utilized for the WGCNA network and module construction. Through automated block-wise analysis, interconnected genes were assigned into 36 color-coded modules, excluding the grey module, which represents uncorrelated genes (Fig. 2). The largest number of co-expressed genes was found

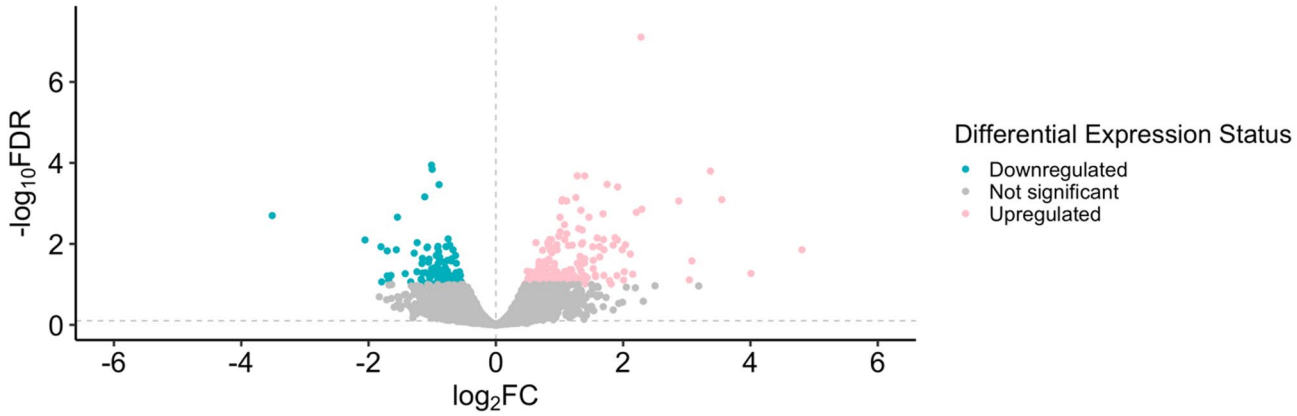


**Fig. 1**. Volcano plot of the differentially expressed genes of the amniotic membrane between mares with ascending placentitis and normal mares (control group). Each dot represents a gene. The y-axis represents the -log10 of the FDR (adjusted p-value) value, and the x-axis represents the log2 FC (fold change) value. Green dots are significantly downregulated genes ($n = 111$), and pink dots are significantly upregulated genes during ascending placentitis ($n = 177$). Grey dots represent genes with an FDR greater than 0.1 that were not considered significantly differentially expressed.

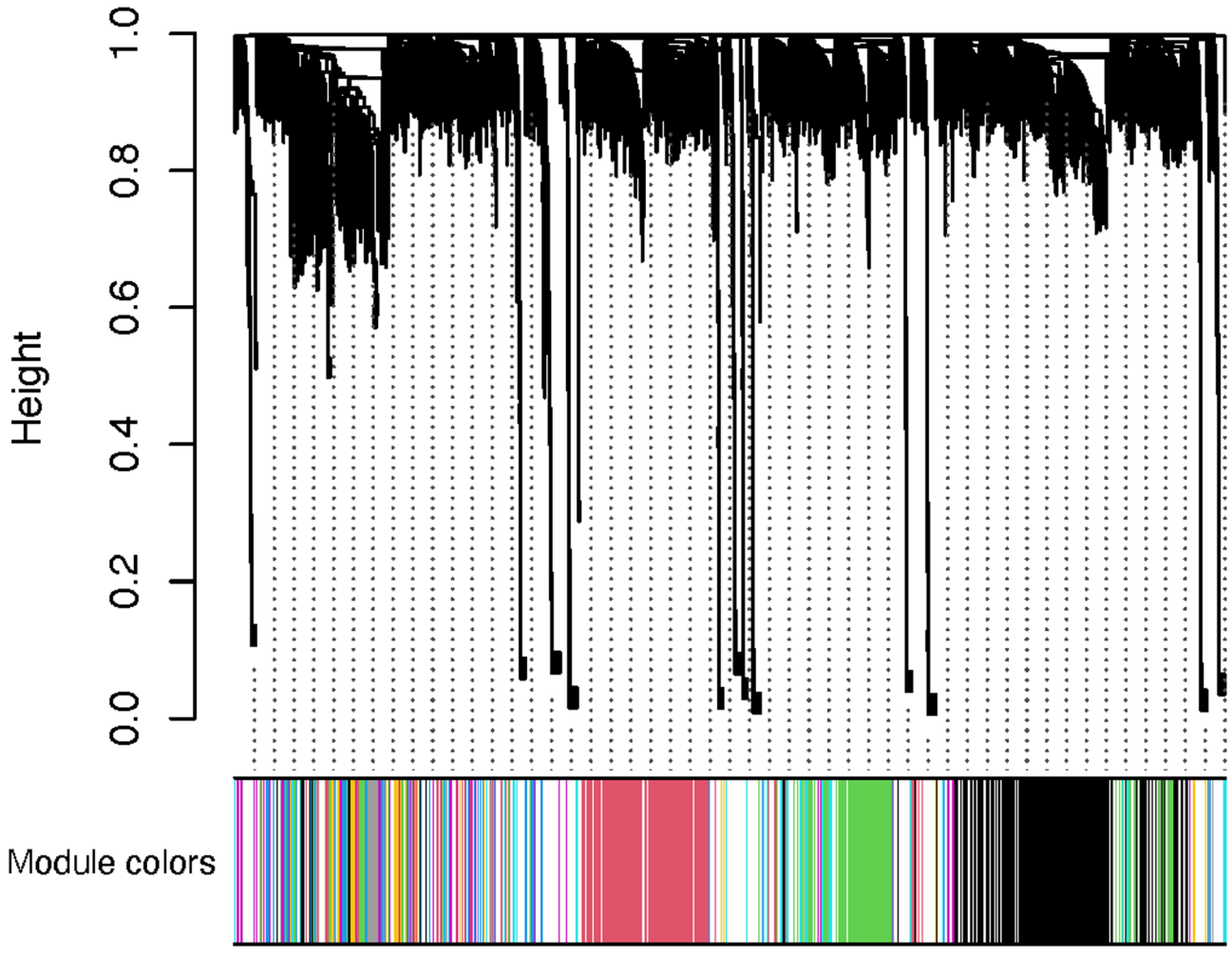


**Fig. 2**. Gene co-expression module dendrogram. Cluster dendrogram of 32,004 genes generated through dissimilarity metrics (1-TOM) and hierarchical clustering. The module colors (x-axis) show the gene-module assignment, and the height (y-axis) represents the dissimilarity between genes.

in the brown module ($n = 2126$), while the dark magenta module had the smallest number of co-expressed genes ($n = 70$) (Supplementary Table S3).

Additionally, a heatmap was generated to assess the relationship between modules and clinical traits (inflammation and placentitis) using the Kendall correlation (Fig. 3). Within 36 modules, "brown" was positively correlated with inflammation ($R = 0.81$, $p = 0.001$) and placentitis ($R = 0.74$, $p = 0.006$) score traits. Module "dark magenta" was negatively correlated with inflammation ($R = -0.7$, $p = 0.01$) and placentitis score traits ($R = -0.7$, $p = 0.01$).

## Functional enrichment

Pathway overrepresentation analysis (PANTHER Overrepresentation Test - PANTHER Pathways and GO-slim biological process)[26] of DEGs demonstrated that genes were predominantly involved (FDR < 0.05) in biological processes linked with Toll-like receptor 4 signaling pathway, cytokine-mediated signaling pathway, and small molecule metabolic process (Supplementary Table S4). Moreover, the overrepresented pathways were the toll receptor signaling pathway (*CD14*, *TLR4*, and *PTGS2*) and CCKR signaling map (*MMP9*, *EIF4EBP1*, *CASP3*, *FOXO3*, *PTGS2*, *TCF4*, *DNM1*, *NR4A1*, and *AKAP1*) (Fig. 4, Supplementary Table S5).

Additionally, we also evaluated the genes of the two highly correlated modules, brown and dark magenta. The PANTHER overrepresentation analysis (PANTHER Pathways and GO-slim biological process)[26] of the genes in the "brown" module were significantly involved in biological processes associated with the Toll-like receptor 4 signaling pathway, canonical NF-κB signal transduction, cytokine-mediated signaling pathway, and others (Supplementary Table S6). Additionally, the analysis revealed three significantly enriched pathways (FDR < 0.05), the toll-like receptor (TLRs) signaling pathway (*IRAK4*, *MAP2K1*, *CD14*, *ECSIT*, *RELA*, *NFKB1*, *TNFAIP3*, *PTGS2*, *TLR4* and *NFKB2)*, glycolysis (*PFKL*, *GAPDH*, *PGK1*, *HK2*, *ENO1*, *ENO2*, and *GPI)*, and interleukin signaling pathway (*IL4R*, *FOXO3*, *IL12A*, *IL13RA1*, *IL16*, *IL10RB*, and *ELK1*) (Fig. 4, Supplementary Table S7).

The PANTHER overrepresentation analysis of the genes in the dark magenta module did not yield any significant (FDR < 0.05) pathways or biological processes.

### Protein-protein interaction

Hub genes from the "brown" module were identified by establishing a cutoff of MM > 0.6 and GS > 0.4, which revealed 1,280 inflammation-associated hub genes. The hub genes list of the "brown" module was overlapped with the list of genes of the Toll-like receptor signaling pathway generated by the overrepresentation analysis. Hub genes of the "brown" module, which were included in the Toll-like receptor signaling pathway list, were used to construct a physical subnetwork protein-protein interaction analysis.

The analysis revealed a significant PPI enrichment score of $P = 1.0e\text{-}16$, comprising 14 nodes (genes) and 16 edges (interactions), with an average node degree of 2.29 and a local clustering coefficient of 0.631 (Fig. 5).

Additionally, the DEG list was used to construct another physical subnetwork protein-protein interaction analysis. The analysis revealed a significant PPI enrichment score of $P = 1.0e\text{-}16$, comprising 264 nodes and 42 edges, with an average node degree of 0.311 and a local clustering coefficient of 0.156 (Supplementary Fig. S1).

## Immunohistochemistry

The protein staining for TLR4 and PTGS2 in the equine amnion from the placentitis and control groups is shown in Fig. 6. According to our DEG findings, we observed an increased expression of *TLR4* and *PTGS2* in the placentitis group compared to the control group. TLR4 was seen in the cytoplasm and nucleus of the epithelial cells, and it also appears in the nucleus of the fibroblasts in the connective tissue. PTGS2 was mainly expressed in the cytoplasm of the epithelial cells. The immunostaining intensity for the evaluated targets was relatively higher in the equine amniotic membrane from the placentitis group than in the control group. In the current RNA sequencing dataset, *TLR4* and *PTGS2* were significantly upregulated in the amniotic membrane (log2FC = 1.0 and log2FC = 1.9, respectively) during placentitis compared with the control (Fig. 6).

No immunostaining was observed in sections incubated with either normal rabbit IgG or the PU.1 antibody, confirming the specificity of the staining observed with TLR4 and PTGS2 antibodies (Supplementary Fig. S4).

## Discussion

The amniotic membrane is the innermost fetal membrane that delimits the amniotic cavity, which contains the amniotic fluid that is in direct contact with the fetus. Changes to the amniotic membrane and the amniotic fluid can negatively impact the fetus's health when transcriptomic dysregulations occur during placentitis. Thus, the current study characterized the gene expression of the amniotic membrane to improve our understanding of the molecular mechanisms and critical regulators involved in ascending placentitis in mares. To perform this study, the amniotic membrane was collected from experimentally induced ascending placentitis models and healthy pregnant mares at 288 days of gestation. High-dimensional biology, specifically RNA sequencing, was applied to characterize the transcriptome of the specific tissue. Combined with updated functional genomics, the study reveals important key regulators and pathways contributing to a better understanding of placentitis' pathophysiology. Our results indicated that the amniotic membrane functions not only as a physical barrier but also actively participates in the immune response by engaging toll-like receptor signaling, promoting inflammatory pathways, and activating glycolysis when challenged by ascending placentitis.

In mammals, healthy pregnancies are maintained by high concentrations of progesterone, downregulating chemokines and blocking the inflammatory cascade at the feto-maternal interface[27–29]. These chemokines and inflammatory factors are activated during normal labor, but they are also triggered by infection, which leads to preterm delivery in mice, women[30,31]and mares[19]. Our study found that equine ascending placentitis leads to the increased expression of genes involved in the inflammatory process in the amniotic membrane, particularly

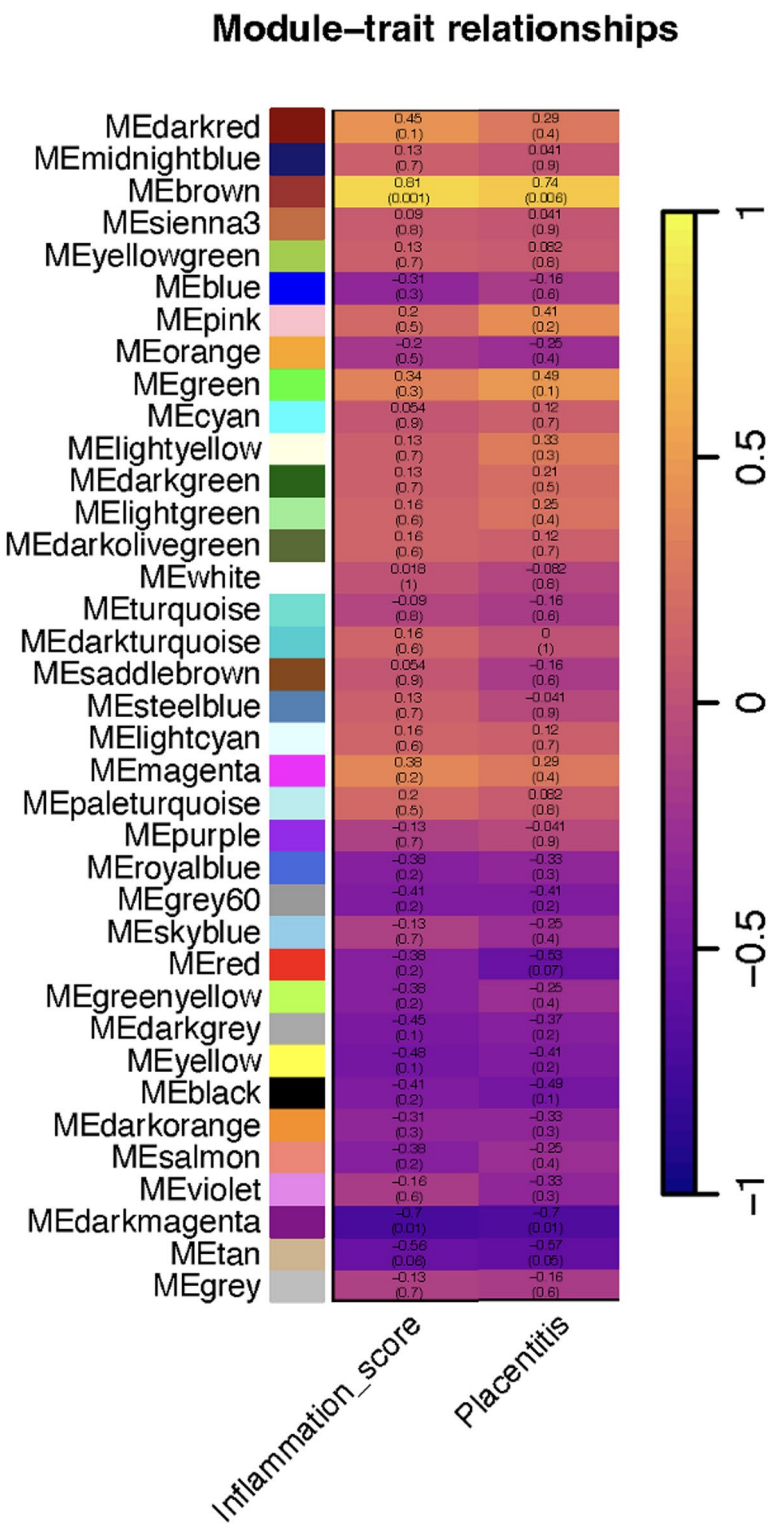


**Fig. 3**. Weighted gene expression co-expression network analysis (WGCNA) of 32,004 genes in the amniotic membrane during ascending placentitis and the identified 37 color-coded modules. Module-trait heatmap based on the relationships between co-expression modules and score traits (Inflammation and Placentitis). The "brown" module was positively correlated with inflammation and placentitis. The "dark magenta" module was negatively correlated with inflammation and placentitis. Each row represents the identified co-expression modules, and each column represents a specific trait. The color yellow indicates a positive correlation between the module and the trait, while the purple color indicates a negative correlation.

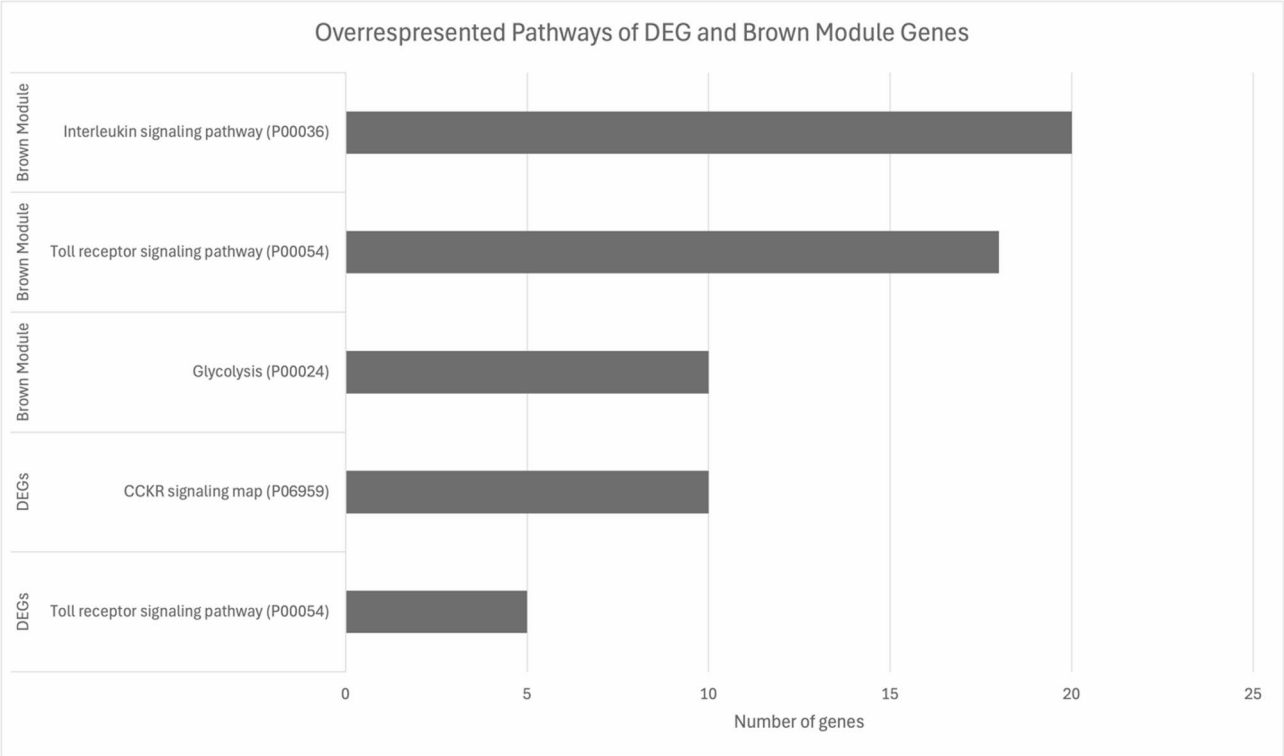


**Fig. 4**. Gene ontology (GO) enrichment analysis using PANTHER was used to identify the overrepresented pathways of the DEGs and the genes from the brown module, which was highly positively correlated with placentitis and inflammation based on the WGCNA analysis. The y-axis contains the pathways with an FDR < 0.05, and the x-axis contains the number of genes assigned in each pathway.

those related to the toll-like receptor signaling pathway. Our findings align with previous studies that evaluated different tissues during ascending placentitis in mares, which also demonstrated the upregulation of genes involved in pathogen recognition and inflammation[19,22,24]. Functional annotation analysis of our results revealed that both DEGs and the brown module genes were enriched in the Toll receptor signaling pathway. Additionally, the DEGs were enriched for inflammation-related processes, such as the CCKR signaling map, and the genes in the brown module were enriched for glycolysis and the interleukin signaling pathway. The analysis of the genes in the dark magenta module did not reveal any significant pathways.

Toll-like receptors (TLRs) are considered pattern recognition receptors (PRRs), which are essential components of the innate immune system[32,33]. They are responsible for recognizing molecular patterns associated with microbial pathogens (Pathogen-Associated Molecular Patterns (PAMPs)) and molecules released by damaged cells (Damage-Associated Molecular Patterns (DAMPs))[32]. Thus, TLRs play an essential role in the immune system. These PAMPs and DAMPs signal infections, activating both inflammatory and antimicrobial responses[34]. In the present study, several TLRs signaling-related genes (*CD14*, *LY96*, *ECSIT*, *TLR4*, *TLR9*, *NFKB2*, *PTGS2*, *NFKB1*, *TNFAIP3*, *TLR8*, *RELA*, *ELK1*, *TLR2*, and *NFKBIA*) were upregulated in the amniotic membrane from mares with ascending placentitis, being hub genes in the "brown" module in the amniotic membrane WGCNA dataset. IHC analysis confirmed the overexpression of TLR4 and PTGS2 in the amniotic membrane of mares with ascending placentitis (Fig. 6). Although histological examination of the amniotic membrane did not reveal inflammatory features (e.g., leukocyte infiltration, edema, or necrosis), transcriptomic analysis identified DEGs related to inflammatory pathways. This finding may reflect an early immune response, in which molecular signaling is activated before structural or cellular changes become histologically evident. Moreover, although *TLR4* is traditionally considered a transmembrane receptor[35]studies have shown its nuclear localization in certain cell types, such as glioblastoma and lung epithelial cells, particularly following inflammatory stimulation[36,37]. In our study, the observed nuclear TLR4 staining in the amniotic membrane may reflect an early immune response. However, further investigation into its functional significance is needed. A recent study has also identified the upregulation of TLRs-related genes (*TLR1*, *TLR2*, *TLR3*, *TLR7*, *MYD88*, *IRAK1*, and *LY96)* in the chorioallantois membrane of mares with ascending placentitis[19]. Similarly, in humans, TLRs are expressed in the amniotic membrane cells and are involved in the active recognition and regulation of intra-amniotic infection[7,33,38]. Specifically, *TLR4*, one of the genes present in the "brown" module and an upregulated DEG, stimulates cytokine release and activates apoptosis pathways, triggering the immune response in women with intra-amniotic infection[38,39]. The predominant upregulation of *TLR4* rather than *TLR2* observed in this study may suggest that the amniotic membrane is not directly exposed to the bacteria, which activates *TLR2* via PAMPs[40]. Instead, the inflammatory response may be driven primarily by DAMPs, which preferentially

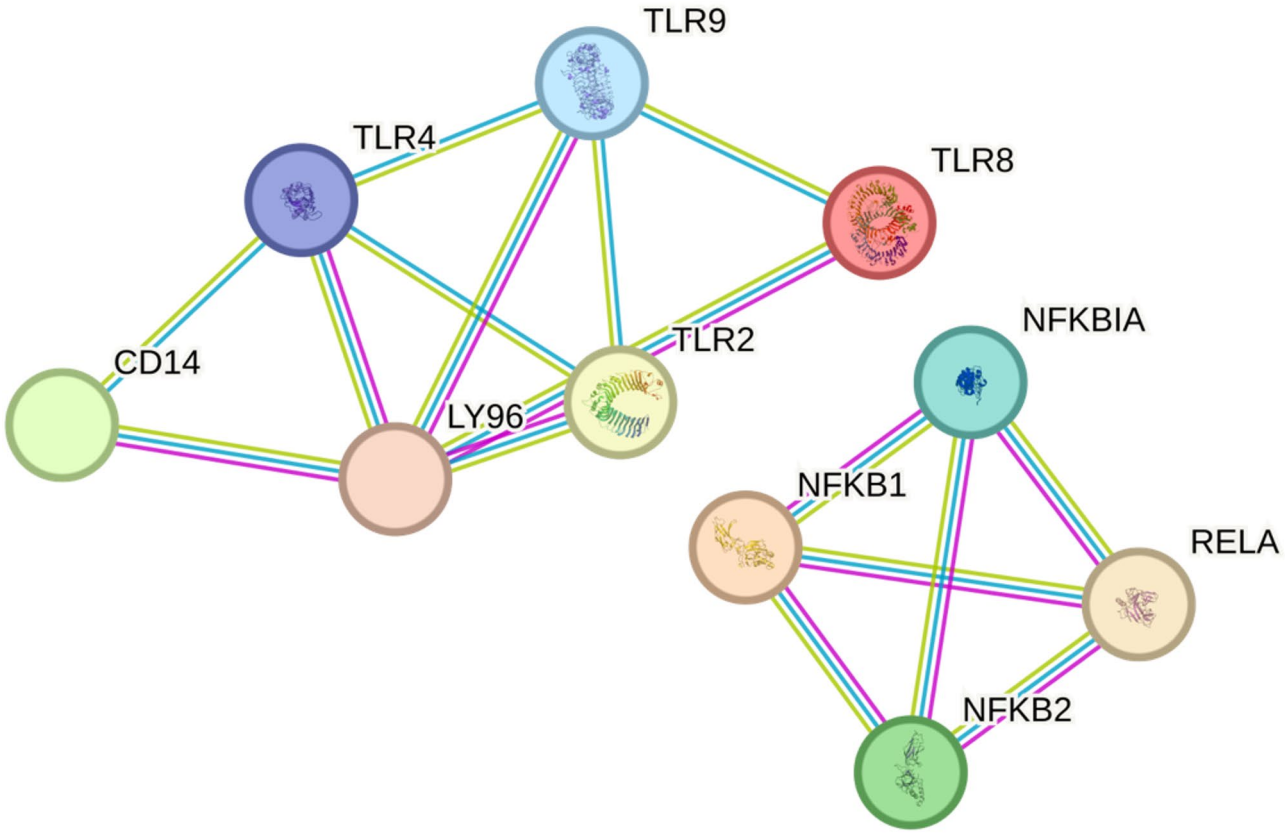


**Fig. 5**. Protein-protein interaction analysis with the STRING algorithm showing nodes (proteins) and edges (protein-protein interactions) of proteins in the Toll-like receptor signaling pathway. A functional interaction network represents the relationships between proteins encoded by genes present in the Toll-like receptor signaling pathway. Thicker edges indicate stronger protein-protein interactions. Each node represents all the proteins produced by a single protein-coding gene locus. Node colors represent query proteins, and the first shell of interactors, and node content indicates known or predicted 3D structure.

activate *TLR4*, which can also be activated through co-receptors such as *CD14* and *LY96* that are shown to be upregulated in our study[41,42]. This suggests that *TLR4*-mediated signaling in the amniotic membrane reflects the downstream consequences of infection rather than direct bacterial recognition. Therefore, our data suggest that TLRs play a crucial role in maintaining the inflammatory response activation during placentitis. In primates, treating intra-amniotic infection using a TLR antagonist has been shown to delay or prevent preterm delivery associated with the infection[43]. Thus, inhibiting TLRs in combination with effective antibiotic therapy may be a promising strategy for developing new therapies for equine ascending placentitis, potentially suppressing the inflammatory response and preventing preterm delivery.

To improve our knowledge of the genes in the brown module most correlated with the TLR signaling pathway (*CD14*, *LY96*, *ECSIT*, *TLR4*, *TLR9*, *NFKB2*, *PTGS2*, *NFKB1*, *TNFAIP3*, *TLR8*, *RELA*, *ELK1*, *TLR2*, and *NFKBIA*), we performed a protein-protein interaction analysis. The functional network generated by STRING revealed interesting interactions among the genes, with strong edges connecting *RELA*, *NFKB1*, and *NFKB2*. It is known that *RELA*, *NFKB1*, and *NFKB2* are essential components of the classic NF-κB family[44]which needs to be suppressed in order to maintain pregnancy in humans[44]. NF-κB is inhibited by certain important cytokines, such as *IL-10*, and also by hormones like progesterone, which are elevated during pregnancy[44–46]. A significant relationship between NF-κB activity, pro-inflammatory cytokines, and preterm birth in women has been discussed, as demonstrated by an *IL-10* knock-out (KO) mouse model[44,47]. The KO of the *IL-10* resulted in increased expression of *IL-6* and *TNF-α*, which promoted preterm labor[47]. In our study, *IL-6* was identified as a hub gene in the "brown" module. Other studies conducted in mares with experimentally induced ascending placentitis, which have analyzed various samples, including the chorioallantois, endometrium, cervix, and fetal fluids, have shown an increase of *IL-6* in all these tissues[3,19,24,48]. The increased expression of *IL-6* in various tissues during ascending placentitis may be evidence of the coordinated immune response across the tissues directly involved in pregnancy. Moreover, in mares with placentitis, the chorioallantois membrane shows a significant downregulation of transcripts involved in the synthesis of 5α-dihydroprogesterone (5αDHP) and several glucocorticoid/steroid hormone receptors[19]. The consequent lower concentration of these important progestins and their function will lead to the activation of the NF-κB pathway, amplifying the inflammatory process involved in the disease[19,49]. Therefore, our study demonstrated that NF-κB plays an important role in

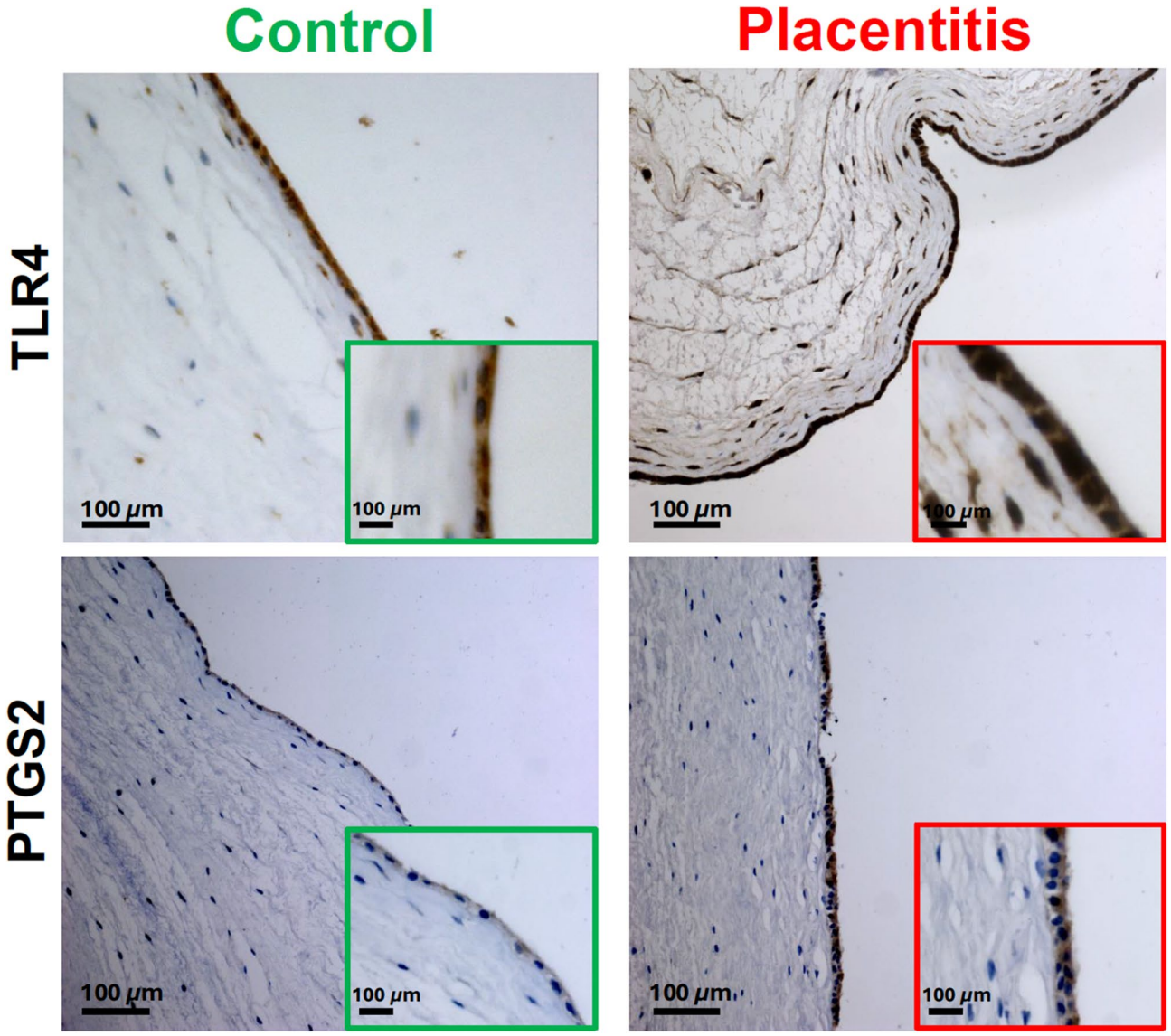


**Fig. 6**. Representative photomicrographs of the equine amniotic membrane retrieved from control and placentitis mares and immunostained for Toll-like Receptor 4 (TLR4) and Prostaglandin-endoperoxide Synthase 2 (PTGS2). The immunostaining intensity for the evaluated proteins was higher in the equine amniotic membrane from the placentitis group than in the control group. Scale bar = 100 $\mu$m.

activating the inflammatory cascade during ascending placentitis, and it may be a promising target for developing new therapies.

The glycolysis pathway was enriched when analyzing the genes in the brown module. This pathway has also been overrepresented in the chorioallantois and endometrium of mares during ascending placentitis[19]. However, there is no currently known direct correlation between those specific glycolytic genes and ascending placentitis. This finding may indicate metabolic adaptations during the disease.

The brown module analysis has also revealed an enrichment in the interleukin signaling pathway. This pathway has also been overrepresented in the myometrium, cervix, and chorioallantois of mares during ascending placentitis[19,22,23]. In our data, the genes driving the pathway were *STAT3*, *CSF2RB*, *FOXO3*, *IL13RA1*, *SPI1*, *IL4R*, *CDKN1A*, *MKNK1*, *IL16*, *IL10RA*, *IL10RB*, *MAP3K4*, *ELK1*, *LOC100069576*, *IL12A*, *IL6*, and *MKNK2*. This pathway is known for mediating inflammatory and immune responses, which may contribute to the pathological changes observed during placentitis. The gene *FOXO3* is part of the family Forkhead box transcript. *FOXO3* expression was higher in the myometrium of women in labor compared to nonlaboring women[50]. In addition, its overexpression increased cytokine synthesis and secretion, prostaglandin production, and *MMP9* expression[50]which we have found to be a DEG upregulated in the amniotic membrane during placentitis. Interleukin 10 Receptor Subunit Beta (*IL10RB*), also known as *IL10R2*, plays a crucial role in the immune system and has been linked to recurrent pregnancy loss in women[51]. The gene *STAT3* is a signal transducer and activator of transcription 3. It is one of the downstream genes activated by *IL6* via the JAK/STAT pathway. It has been

shown that *IL6* plays an important role as a pro-survival agent during ascending placentitis[52]. However, *STAT3*, one of the triggered genes activated by *IL6*, is expressed in the myometrium as an upstream regulator during the prepartum period in mares, indicating its involvement in labor signals[22]. Thus, it raises the question of whether *IL6* might accelerate labor by activating the myometrium through *STAT3* signaling. Overall, genes involved in the interleukin signaling pathway may not only have a role in triggering the inflammatory response but also in producing further signals that might continuously stimulate the inflammation process and, consequently, signal parturition. Thus, it is an important pathway that warrants further investigation as a potential target for developing new therapeutic strategies to prevent preterm delivery in mares when in conjunction with an antimicrobial therapy.

When evaluating the overrepresentation analysis for the DEGs, we observed an enriched pathway known as the CCKR signaling map. While there is no published correlation between this pathway and ascending placentitis, several genes within this pathway are associated with the inflammatory process during placentitis in mares in other tissues, including *MMP9*, *CASP3*, *FOXO3*, *PTGS2*, and *NR4A1*[19,22,23]. The gene *MMP9* is a potent coding gene for proteinases, which may be involved in extracellular matrix degradation and has been identified as being involved in cervical remodeling during ascending placentitis in mares[23,24,53]. This elevated protease transcript can be associated with apoptosis[54]. In support of this, the gene *CASP3*, an important apoptosis-related gene, was identified as a hub gene ("brown" module) and overexpressed in the amniotic membrane of mares with placentitis. *CASP3* is a major member of the caspase family and plays an active role in apoptosis, acting as a high-risk factor for premature membrane rupture in women[55]. In line with our findings, *CASP3* has shown up as an upstream regulator in the chorioallantois of mares with ascending placentitis and is upregulated in the cervix of mares during the disease[19,23,24]. Data suggests that genes related to apoptosis may be involved in the observed placental separation during equine placentitis[19]. Thus, controlling apoptosis-related genes may prevent premature placental separation and cellular apoptosis in mares.

A recent study has characterized the downregulation of factors involved in progestin synthesis and function during placentitis in mares[19]. In accordance with their data, our study has also identified the downregulation of an important glucocorticoid/steroid hormone receptor, the *NR4A1*, in the amniotic membrane of mares with placentitis. It implicates progestin functional withdrawal, which may contribute to the activation of inflammatory cascades[19]. Moreover, El-Sheikh Ali and colleagues have demonstrated that placentitis is associated with angiogenesis dysregulation due to the downregulation of angiogenesis-related genes (*VEGFA*, *VEGFR2*, and *VEGFR3)* in the chorioallantois of mares with placentitis[19]. In line with their observations, we have also identified hypoxia-related genes (*SOD2*, *BNIP3*, and *HMOX1*) upregulated in the amniotic membrane of mares with placentitis. Consequently, these findings may elucidate the occurrence of placental insufficiency in cases of ascending placentitis.

Additionally, the functions of the amniotic membrane remain to be fully understood. A recent study found a similar structure to lamellar bodies inside epithelial cells in the amniotic membrane[56]. Lamellar bodies are lamellated structures that store surfactants. They are commonly produced by type II pneumocytes in the fetal lung and then are secreted in the amniotic fluid[57,58]. This possible function of the amniotic membrane suggests it might be a potential source of pulmonary surfactant in the amniotic fluid[56,59]. Thus, it raises the hypothesis that any disturbance in the amniotic membrane, such as we have shown that happens during ascending placentitis, could lead to direct harm to the fetus. Even though foals from chronic placentitis tend to be precociously mature and are more likely to survive, their future health and athletic performance might be compromised, leading to significant economic consequences[3].

Compared to the most recent reports that evaluated the transcriptome in other reproductive tissues, the amniotic membrane presented fewer DEGs (288 genes) than the cervix (5310 DEGs)[23,24]myometrium (596 DEGs)[22]endometrium (805 DEGs), and chorioallantois (2953 DEGs)[19] from mares with placentitis. We hypothesize that the smaller list of DEGs in the amnion can be correlated with the relatively fewer cell types and presumed reduced vascularization compared to other placental tissues, which may contribute to this tissue's lower metabolic activity and immune response[56]. Indeed, the amniotic membrane expresses genes with similar patterns to other tissues. An inflammation-driven remodeling was observed in the cervix, characterized by the upregulation of important PRRs, interleukins, and proteases that contribute to extracellular matrix degradation[23,24]. Similar results were observed in the myometrium, including genes involved in prostaglandin synthase and apoptosis[22]. The endometrium and chorioallantois followed the same patterns, additionally showing the downregulation of progestin functional withdrawal[19]. Most of these previously published DEGs and patterns were also observed in the amniotic membrane during ascending placentitis (Fig. 7). Additionally, a more in-depth comparison (Supplementary Table S8 and Supplementary Fig. S3) revealed eight genes upregulated in all the tissues during ascending placentitis (*AOAH*, *SOD2*, *LOC100053579*, *ITGAX*, *LOC100067491*, *CEBPD*, *IL2RG*, *OAF*). Together, these genes reflect a coordinated inflammatory response across all placental tissues and myometrium, including innate immune response activation, redox imbalance, and cytokine signaling[60,61]. Moreover, some genes were only expressed in the amniotic membrane when compared to other tissues, with 42 being upregulated and 43 being downregulated (Supplementary Fig. S3).

A few limitations must be considered. The relatively small sample size ($n=6$ per group) may limit the statistical power to detect subtle changes. However, previous research has demonstrated that six biological replicates per experimental group for bulk RNA sequencing is an adequate minimum threshold for estimating gene-level dispersion, biological coefficient of variation, and differential expression, particularly when the average sequencing depth surpasses 20 million reads per sample[62–66]. Moreover, the methodology and subsequent delineation of differential gene expression used in this work are considered somewhat conservative, intentionally controlling for the apparent false positive rate. Another limitation of our study is that it did not explore single-cell RNA sequencing. However, this approach would be valuable for identifying which amnion cell types drive the observed transcriptomic changes. Therefore, future studies that implement single-cell RNA

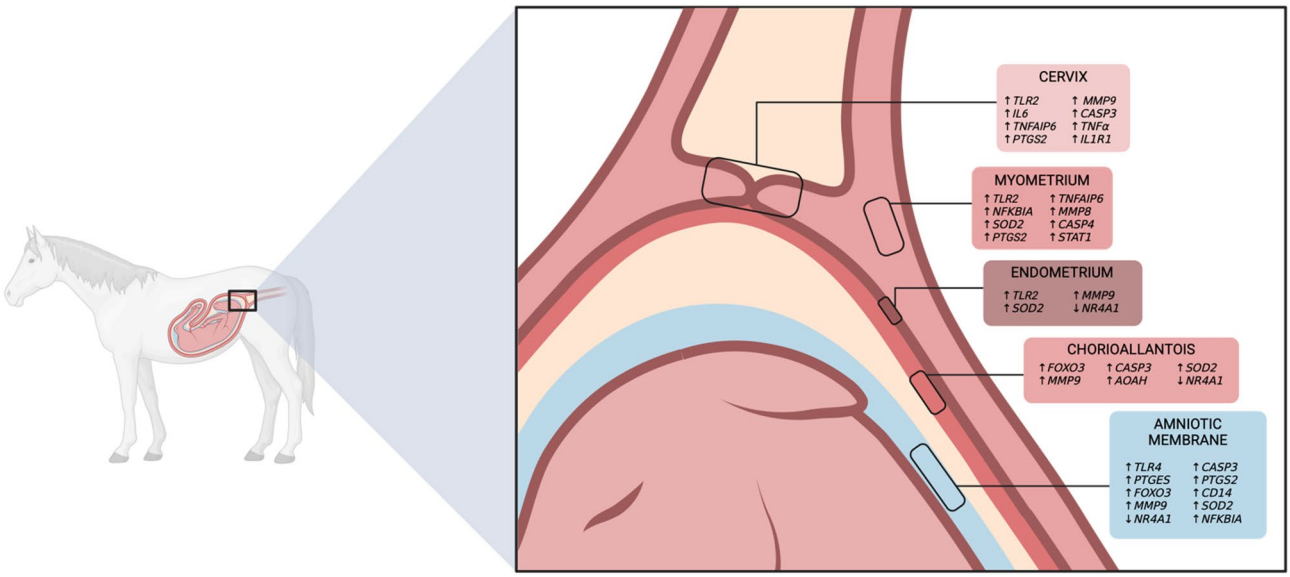


**Fig. 7**. Graphical representation of the gene expression throughout the tissues mainly involved in pregnancy. Inflammation-driven remodeling, interleukins, and apoptosis-related genes were observed in the cervix, and pattern recognition receptors, oxidative stress, apoptosis, decreased angiogenesis, and progestin functional withdrawal-related genes were affected in the myometrium, endometrium, and chorioallantois. Those genes were also expressed in the amniotic membrane, showing a coordinated immune response across all the tissues[19,22–24]. *Created in BioRender. Marchio, S. (2025)*https://BioRender.com/6nfo956.

sequencing, complementary quantitative methods, and a larger sample size may be worthwhile to further elucidate transcriptomic alterations or disruptions caused by ascending placentitis in mares. Lastly, the use of an experimentally induced model of ascending placentitis is a valuable tool for controlling variables and the timing of infection. However, it may not fully replicate the complexity and variability of naturally occurring disease. Despite these limitations, it is worth noting that this experimentally induced model of ascending placentitis currently represents the most suitable model for studying the disease's mechanisms under controlled conditions. It has been previously validated and widely used, generating relevant biological evidence[10,19,22,23].

In conclusion, this is the first study that elucidated the changes in the equine amniotic membrane during ascending placentitis (Fig. 8). Our study highlights that the amniotic membrane is not only a physical barrier but also plays an active role in the immune response during ascending placentitis. We observed an inflammatory response triggered mainly by TLRs, which may subsequently activate genes involved in prostaglandin synthesis (*PTGS2* and *PTGES*), apoptosis (*MMP9* and *CASP3*), and hypoxia (*SOD2*, *BNIP3*, and *HMOX1*). The expression of all these factors in the amniotic membrane can be a consequence of the immune response in other tissues. Still, more importantly, it will contribute to the perpetuation and exacerbation of the inflammatory response in various tissues, leading to placental insufficiency, premature placental separation, and preterm delivery. The amniotic membrane participates in immune crosstalk with the surrounding tissues mentioned above, including the myometrium, endometrium, and chorioallantois. However, further studies will be necessary to elucidate the role of the amniotic membrane in contributing to the composition of amniotic fluid and fetal health. Altogether, this study revealed the amniotic membrane transcriptome during ascending placentitis and contributed to understanding the pathophysiology of placentitis. Additionally, our results can also serve as a consistent source for testing new hypotheses.

## Materials and methods

### Ethics

All experimental protocols and sample collections were approved by the Institutional Animal Care and Use Committee at the University of Kentucky (IACUC protocol number 2014 – 1341). All methods were carried out in accordance with relevant guidelines and regulations in the manuscript. All methods are reported in accordance with the ARRIVE guidelines.

### Animals

Healthy mares (*Equus caballus*), from the University of Kentucky, Maine Chance Farm, with no detectable abnormalities in the reproductive tract, were enrolled in the study. Animals were maintained at the University of Kentucky Maine Chance Farm in pastures with *ad libitum* access to water, hay, and trace minerals. They were 4.39 ± 0.18 years old (mean ± SEM; range: 4–6 years). Mares were housed with a fertile 4-year-old stallion for 45 days to allow live cover. Between 18 and 35 days of gestation, pregnancy diagnoses were made with a transrectal ultrasonographic exam, and subsequent embryo measurements were used to predict pregnancy length[67].

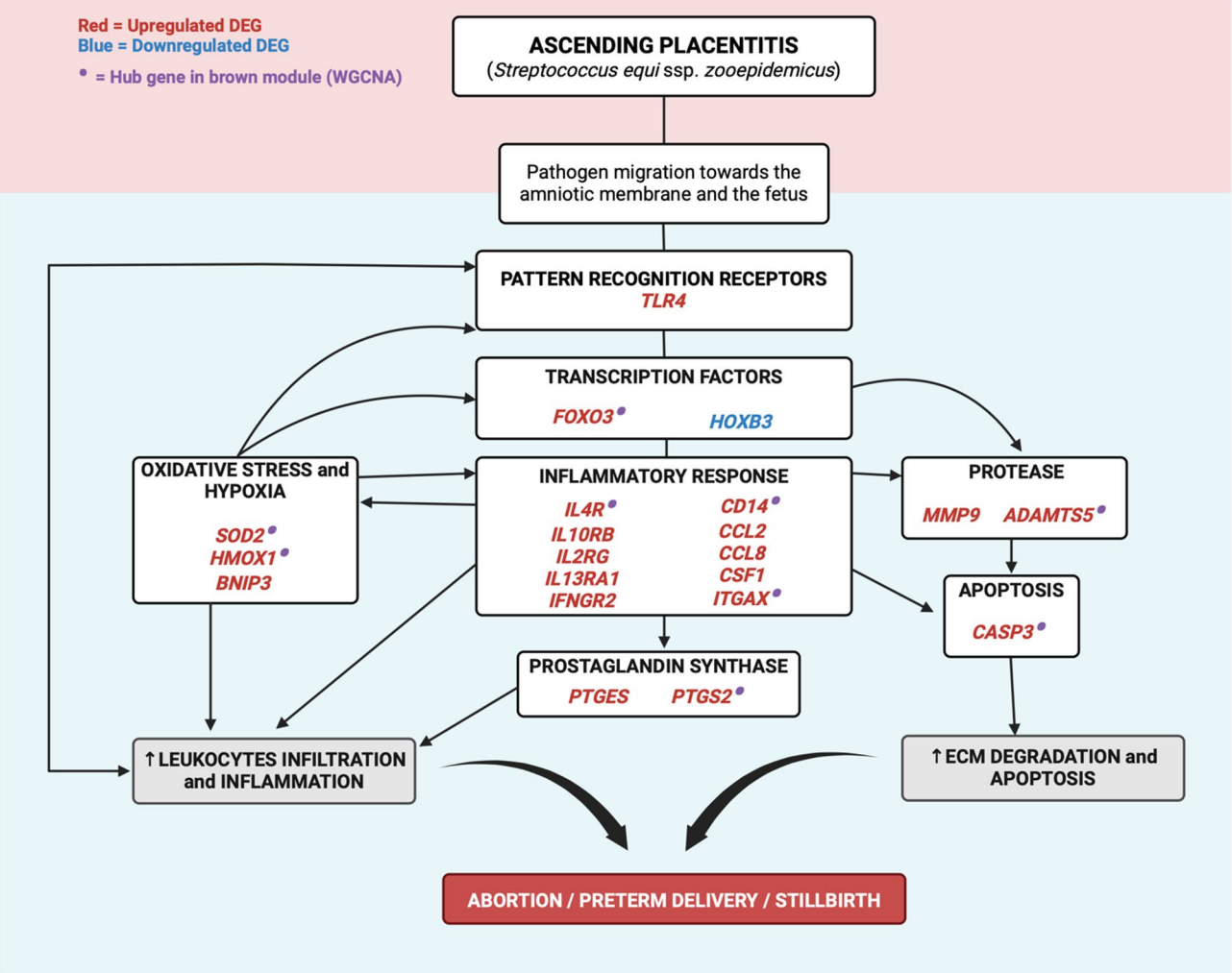


**Fig. 8**. Graphical representation explaining the possible mechanisms associated with equine placentitis in light of the current study. *Created in BioRender. Marchio, S. (2025)*https://BioRender.com/6nfo956.

## Experimental design

At approximately 280 days of gestation age, mares were randomly divided into two groups: placentitis ($n=6$ mares) and control ($n=6$ mares) groups. An intracervical inoculation of *Streptococcus equi* ssp. *zooepidemicus* ($1\times10^6$ CFU) diluted in 0.5 ml of Todd Hewitt broth, using a semiflexible artificial insemination pipette, was done to experimentally induce placentitis. No inoculation was performed on the mares in the control group. All mares were monitored daily thereafter by transrectal ultrasonographic examination to evaluate the CTUP (Supplementary Fig. S2) and to assess the degree of placental separation, which indicated the progression of disease[5,9].

## Euthanasia and placental tissue collection and preparation

Eight days after inoculation, mares in the placentitis group presented measurable placental separation and a noticeable increase in CTUP (CTUP increase of 3 mm and > 50% of original thickness)[5,10] and were euthanized as described elsewhere[19]. Briefly, an overdose of sodium pentobarbital recommended by the American Veterinary Medical Association (AVMA) was utilized[68]. Mares in the control group were euthanized at corresponding gestational ages with the same protocol recommended by the AVMA (sodium pentobarbital overdose). Immediately after euthanasia, the uteroplacental unit was retrieved. Swabs from active placentitis lesions were taken and cultured on blood agar plates (incubated at 37 °C) to confirm the isolation of *Streptococcus equi* ssp. *zooepidemicus* from the lesion.

Since there were no gross lesions in the amniotic membrane, small tissue fragments were randomly collected from each mare and stored in RNAlater (#AM7021; Invitrogen) at 4 °C overnight, followed by freezing at -80 °C until RNA isolation. Samples of amniotic membrane and full-thickness uterus, including chorioallantois (CA), were fixed in 10% formaldehyde for 24 h and then transferred to 100% methanol for histopathological examination of the full-thickness uterus with CA and immunohistochemistry (IHC) of the amniotic membrane.

The histopathological examination of the full-thickness uterus and CA was used only to identify inflammation and confirm placentitis.

### Total RNA extraction

The RNA extraction was done as previously described[19]. In brief, total RNA was isolated using the RNeasy Mini Kit (#74104; Qiagen), and DNA digestion was done on-column utilizing RNase-free DNase I (#79254: Qiagen), followed by cleanup. All procedures were performed according to the manufacturer's instructions. The RNA purity was evaluated with the NanoPhotometer spectrophotometer (IMPLEN, CA, USA), and its integrity and quantification were assessed with the RNA Nano 6000 Assay Kit of the Bioanalyzer 2100 system (Agilent Technologies, CA, USA). All samples had a 260/280 ratio > 2.0 and RNA integrity number (RIN) > 6 (6.47 ± 0.29, mean ± SEM).

### RNA sequencing

All amniotic membrane samples were submitted for RNA sequencing, which was performed at the Novogene Experimental Department as described elsewhere[69–72]. A total of 1 µg of RNA per sample was used as input material for the RNA sample preparations. Sequencing libraries were generated by the NEBNext Ultra RNA Library Prep Kit for Illumina (NEB, USA) according to the manufacturer's protocol, and index codes were added to attribute sequences to each sample. Poly-T oligo-attached magnetic beads were employed to purify mRNA from the total RNA. Fragmentation was done by applying divalent cations under elevated temperature in NEBNext First Strand Synthesis Reaction Buffer (5x). The first strand of complementary DNA (cDNA) was synthesized with random hexamer primers after the fragmentation, followed by the second strand of cDNA synthesis. The directional library was ready after end repair, A-tailing, adapter ligation, size selection, USER enzyme digestion, amplification, and purification. Furthermore, the library was checked using Qubit, while real-time PCR was used for quantification, and a bioanalyzer was used for distribution detection. Quantified libraries were pooled and sequenced on the Illumina NovaSeq 6000 platform (Illumina), generating 150 bp paired-end reads.

### RNA sequencing data normalization

The quality of the sequence read files was assessed by FastQC v0.12.0, and the data was trimmed with Trimmomatic v0.39[73,74]. Reads were mapped to EquCab3.0[75], and a gene-level assembly was performed via an HISAT2 and StringTie2 workflow[76,77]. The gene-level count matrix was constructed utilizing prepDE.py[78]. Raw gene counts were imported to R v4.1.2 and filtered for zero-counts, normalized with the trimmed mean of M-values method (TMM), and then converted into log2-counts-per-million values (log2CPM). A total of 32,004 genes were identified and utilized for weighted network analysis. The RNA sequencing data was deposited in the National Center for Biotechnology Information (NCBI) Gene Expression Omnibus (GEO) database under the number GSE295055.

### Differentially expressed genes

Following normalization with the TMM method, normalized gene count values were used to test for differentially expressed genes (DEGs) in the amniotic membrane between the placentitis and control groups. This evaluation was performed using the R package edgeR v4.0.3 with the function exactTest, which is an exact test based on the negative binomial model. Genes were considered significantly differentially expressed if the raw P-value was < 0.0024[79].

### Comparison of DEGs across other tissues

Using the supplementary materials of previously published papers that were performed with the same experimentally induced placentitis model as our study, we compared the DEGs across the chorioallantois[19]endometrium[19]myometrium[22]and amniotic membrane. Only DEGs with FDR < 0.05 were selected (Supplementary Table S8) and compiled to construct the Venn diagrams (Supplementary Fig. S3).

### Weighted gene co-expression analysis (WGCNA)

First, we evaluated the samples for potential outlier data utilizing canonical Euclidean distance-based network adjacency matrices based on standardized connectivity[80]. Samples with a standardized connectivity >-5.0 were considered outliers and to be removed; no samples were considered outliers for this study. Weighted gene co-expression network analysis was performed with the R package WGCNA v.1.71 for expression network and module construction[81]. According to signed biweight midcorrelation coefficients, the 32,004 genes were constructed into co-expression modules using the blockwiseModules function in the WGCNA R package with the parameters: corType = "bicor," TOMType = "signed," networkType = "signed," maxBlockSize = 32,004, minModuleSize = 30, mergeCutHeight = 0.25, and pamRespectsDendro = FALSE, power = 22, numericLabels = TRUE; prior soft thresholding allowed for the calculation of the power parameter (β) required to exponentially raise the adjacency matrix, targeting a scale-free topology fitting index (R2) of > 90% (β = 22). Each module was assigned to have unique color identification, and genes that did not assemble into a specific module were placed in the "grey" module. Independent module-trait Kendall's Tau correlation coefficients were calculated across all modules and clinical metadata (clinical metadata is available in Supplementary Table S1) components, which were considered significant at $|R| \geq 0.6$ and p-value ≤ 0.05.

After identifying modules strongly positively and negatively correlated with inflammation, we determined their hub genes. Hub genes are highly connected genes within a co-expression network module that often serve as key regulators of biological processes due to their strong association with clinical traits[82]. As such, we calculated the module membership (MM; Kendall's Tau correlation coefficients between gene expression and

module eigengenes as a parameter of intramodular connectivity)[83] and gene significance (GS; Kendall's Tau correlation coefficients between individual gene expression level and clinical trait (inflammation score) as a measure of biological relevance)[84] using the WGCNA R package. Genes that presented MM > 0.6 and GS ≥ 0.4 were considered hub genes within the module.

Genes identified as intramodular hub genes in the brown module, which drive the toll receptor signaling pathway, were further analyzed for protein-protein interactions using the Search Tool for the Retrieval of Interacting Genes database (STRING) with annotations specific to the equine (*Equus caballus*) species. A physical subnetwork was generated in which edges only display protein interactions with evidence of forming a physical complex. No interactions with a confidence score below 0.4 were included, and the disconnected nodes were removed from the network.

### Functional enrichment analysis

Overrepresentation analysis using PANTHER v18.0 was employed to functionally annotate genes based on Gene Ontology (GO) terms, specifically biological processes and pathways. First, we evaluated the list of differentially expressed genes. Then, we evaluated the genes of the "brown" and "dark magenta" modules, which were respectively considered positively and negatively correlated with inflammation ($|R| \geq 0.6$ and p-value $\leq 0.05$). Only pathways with false discovery rate (FDR) adjusted P value < 0.05 were considered.

### Tissue preparation for histopathological examination and immunohistochemical staining

For the histological examination, fixed full-thickness uterus and CA samples were dehydrated, embedded in paraffin, sectioned at 5 µm, and stained with hematoxylin and eosin. The inflammation score was calculated based on the level of inflammation present in the placenta and was graded as 0 (no inflammation; no inflammatory cells), 1 (mild inflammation; few inflammatory cells infiltration), 2 (moderate inflammation; moderate inflammatory cells infiltration), and 3 (marked inflammation; large numbers of inflammatory cells)[19]. Three different high-power fields were utilized to calculate the average score for each sample.

For IHC, fixed amniotic membrane samples were dehydrated, embedded in paraffin, and sectioned at a thickness of 5 µm. The genes of interest were selected based on the results of the RNA sequencing analysis. Briefly, the DEGs list was overlapped with the hub genes (MM > 0.6 and GS > 0.4) list of the "brown" module, which showed a high correlation with placentitis (cor = 0.69 and *P*-value < 1e-200). This correlation was enriched for the Toll-like receptor pathway in the over-representation analysis in PANTHER. Two genes with a P-value of less than 0.0024 were selected for IHC analysis related to inflammation: TLR4 and PTGS2.

The formalin-fixed samples were dehydrated, embedded in paraffin using standard methods, and sectioned at a thickness of 5 µm. The immunostaining of sectioned tissues was conducted with rabbit anti-human TLR4 (1:200; #PA5-23284, ThermoFisher Scientific) or rabbit anti-human PTGS2 (1:100; MA5-14568, ThermoFisher Scientific). Paraffin sections were processed by the Leica BOND-MAX system (Leica Microsystems, Buffalo Grove, IL), as described elsewhere[85]. Slides were evaluated at 100x and 200x magnification.

Negative controls included an omission control using normal rabbit IgG (sc-2027, Santa Cruz Biotechnology) and a substitution control using SPI1 (PU.1) antibody (1:100, PA5-17505, Thermo Fisher Scientific), both applied to equine amnion sections following the same immunohistochemistry protocol as the experimental antibodies.

## Data availability

The RNA sequencing data were deposited in the National Center for Biotechnology Information (NCBI) Gene Expression Omnibus (GEO) database under the number GSE295055, or contact Dr. Yatta Boakari at yboakari@tamu.edu.

Received: 18 April 2025; Accepted: 18 August 2025
Published online: 21 August 2025

## References

1. Giles, R. C. et al. Causes of abortion, stillbirth, and perinatal death in horses: 3,527 cases (1986–1991). *J. Am. Vet. Med. Assoc.* **203**, 1170–1175. https://doi.org/10.2460/javma.1993.203.08.1170 (1993).
2. Hong, C. B. et al. Etiology and pathology of equine placentitis. *J. Vet. Diagn. Invest.* **5**, 56–63. https://doi.org/10.1177/104063879300500113 (1993).
3. Fedorka, C. E. et al. The feto-maternal immune response to equine placentitis. *Am. J. Reprod. Immunol.* **82**, e13179. https://doi.org/10.1111/aji.13179 (2019). https://doi.org/.
4. Cantón, G. J. et al. Equine abortion and stillbirth in california: A review of 1,774 cases received at a diagnostic laboratory, 1990–2022. *J. Vet. Diagn. Invest.* **35**, 153–162. https://doi.org/10.1177/10406387231152788 (2023).
5. Renaudin, C. D., Troedsson, M. H. T., Gillis, C. L., King, V. L. & Bodena, A. Ultrasonographic evaluation of the equine placenta by transrectal and transabdominal approach in the normal pregnant mare. *Theriogenology* **47**, 559–573. https://doi.org/10.1016/S0093-691X(97)00014-9 (1997).
6. Canisso, I. F. et al. Changes in maternal androgens and oestrogens in mares with experimentally-induced ascending placentitis. *Equine Vet. J.* **49**, 244–249. https://doi.org/10.1111/evj.12556 (2017).
7. Abrahams, V. M. et al. Bacterial modulation of human fetal membrane toll-like receptor expression. *Am. J. Reprod. Immunol.* **69**, 33–40. https://doi.org/10.1111/aji.12016 (2013). https://doi.org/.
8. Boakari, Y. L. et al. Serum amyloid A, serum amyloid A1 and haptoglobin in pregnant mares and their fetuses after experimental induction of placentitis. *Anim. Reprod. Sci.* **229**, 106766. https://doi.org/10.1016/j.anireprosci.2021.106766 (2021). https://doi.org/.
9. Canisso, I. F. et al. Serum amyloid A and haptoglobin concentrations are increased in plasma of mares with ascending placentitis in the absence of changes in peripheral leukocyte counts or fibrinogen concentration. *Am. J. Reprod. Immunol.* **72**, 376–385. https://doi.org/10.1111/aji.12278 (2014).
10. Loux, S. C. & Ball, B. A. The proteome of fetal fluids in mares with experimentally-induced placentitis. *Placenta* **64**, 71–78. https://doi.org/10.1016/j.placenta.2018.03.004 (2018). https://doi.org/https://doi.org/

11. LeBlanc, M., Macpherson, M. & Sheerin, P. Ascending placentitis: what we know about pathophysiology, diagnosis, and treatment. *Lexington Am. Assoc. Equine Pract. (AAEP)* **50**, 127–143 (2008).
12. Cummins, C., Carrington, S., Fitzpatrick, E. & Duggan, V. Ascending placentitis in the mare: A review. *Ir. Vet. J.* **61**, 307–313. https://doi.org/10.1186/2046-0481-61-5-307 (2008).
13. Lyle, S. K. Immunology of infective preterm delivery in the mare. *Equine Vet. J.* **46**, 661–668 (2014).
14. Gomez-Lopez, N. et al. RNA sequencing reveals diverse functions of amniotic fluid neutrophils and monocytes/macrophages in intra-amniotic infection. *J. Innate Immun.* **13**, 63–82. https://doi.org/10.1159/000509718 (2020).
15. Motomura, K. et al. RNA sequencing reveals distinct immune responses in the chorioamniotic membranes of women with preterm labor and microbial or sterile intra-amniotic inflammation. *Infect. Immun.* **89**. https://doi.org/10.1128/iai.00819-20 (2021).
16. Pereyra, S., Sosa, C., Bertoni, B. & Sapiro, R. Transcriptomic analysis of fetal membranes reveals pathways involved in preterm birth. *BMC Med. Genom.* **12**, 53. https://doi.org/10.1186/s12920-019-0498-3 (2019).
17. Underhill, L. A., Mennella, J. M., Tollefson, G. A., Uzun, A. & Lechner, B. E. Transcriptomic analysis delineates preterm prelabor rupture of membranes from preterm labor in preterm fetal membranes. *BMC Med. Genom.* **17**, 72. https://doi.org/10.1186/s12920-024-01841-7 (2024).
18. Tissarinen, P. et al. Elevated human placental heat shock protein 5 is associated with spontaneous preterm birth. *Pediatr. Res.* **94**, 520–529. https://doi.org/10.1038/s41390-023-02501-9 (2023).
19. El-Sheikh Ali, H. et al. Transcriptomic analysis of equine placenta reveals key regulators and pathways involved in ascending placentitis. *Biol. Reprod.* **104**, 638–656. https://doi.org/10.1093/biolre/ioaa209 (2020).
20. Pozor, M. Equine placenta – a clinician's perspective. Part 1: normal placenta – physiology and evaluation. *Equine Vet. Educ.* **28**, 327–334. https://doi.org/10.1111/eve.12499 (2016).
21. Turco, M. Y. & Moffett, A. Development of the human placenta. *Development* **146**, dev163428. https://doi.org/10.1242/dev.163428 (2019).
22. El-Sheikh Ali, H. et al. Transcriptomic analysis reveals the key regulators and molecular mechanisms underlying myometrial activation during equine placentitis. *Biol. Reprod.* **102**, 1306–1325. https://doi.org/10.1093/biolre/ioaa020 (2020).
23. El-Sheikh Ali, H. et al. Equine cervical remodeling during placentitis and the prepartum period: A transcriptomic approach. *Reproduction* **161**, 603–621. https://doi.org/10.1530/rep-21-0008 (2021).
24. Fernandes, C. B. et al. Uterine cervix as a fundamental part of the pathogenesis of pregnancy loss associated with ascending placentitis in mares. *Theriogenology* **145**, 167–175. https://doi.org/10.1016/j.theriogenology.2019.10.017 (2020). https://doi.org/.
25. Fernandes, C. B. et al. Upregulation of inflammatory cytokines is associated with alteration in prostaglandin pathways and sex-steroid receptors in the cervix of mares with placentitis. *J. Equine Veterinary Sci.* **66**, 226. https://doi.org/10.1016/j.jevs.2018.05.113 (2018).
26. Mi, H., Muruganujan, A., Casagrande, J. T. & Thomas, P. D. Large-scale gene function analysis with the Panther classification system. *Nat. Protoc.* **8**, 1551–1566. https://doi.org/10.1038/nprot.2013.092 (2013).
27. Bukowski, R. et al. Onset of human preterm and term birth is related to unique inflammatory transcriptome profiles at the maternal fetal interface. *Peer J.* **5**, e3685 (2017).
28. Fedorka, C. E. et al. Alterations in T cell-related transcripts at the feto-maternal interface throughout equine gestation. *Placenta* **89**, 78–87. https://doi.org/10.1016/j.placenta.2019.10.011 (2020). https://doi.org/https://doi.org/
29. Wagner, L. H. et al. Low progesterone concentration in early pregnancy is detrimental to conceptus development and pregnancy outcome in horses. *Anim. Reprod. Sci.* **257**, 107334. https://doi.org/10.1016/j.anireprosci.2023.107334 (2023). https://doi.org/.
30. Biggar, R. J., Poulsen, G., Melbye, M., Ng, J. & Boyd, H. A. Spontaneous labor onset: is it immunologically mediated? *Am. J. Obstet. Gynecol.* **202**, 268. https://doi.org/10.1016/j.ajog.2009.10.875 (2010). .e261-268.e267.
31. Migale, R. et al. Modeling hormonal and inflammatory contributions to preterm and term labor using uterine Temporal transcriptomics. *BMC Med.* **14**, 86. https://doi.org/10.1186/s12916-016-0632-4 (2016).
32. Amarante-Mendes, G. P. et al. Pattern recognition receptors and the host cell death molecular machinery. *Front. Immunol.* **9**. https://doi.org/10.3389/fimmu.2018.02379 (2018).
33. Šket, T., Ramuta, T. Ž., Starčič Erjavec, M. & Kreft, M. E. The role of innate immune system in the human amniotic membrane and human amniotic fluid in protection against intra-amniotic infections and inflammation. *Front. Immunol.* **12**. https://doi.org/10.3389/fimmu.2021.735324 (2021).
34. Medzhitov, R. Toll-like receptors and innate immunity. *Nat. Rev. Immunol.* **1**, 135–145. https://doi.org/10.1038/35100529 (2001).
35. Mineev, K. S. et al. Spatial structure of TLR4 transmembrane domain in bicelles provides the insight into the receptor activation mechanism. *Sci. Rep.* **7**, 6864. https://doi.org/10.1038/s41598-017-07250-4 (2017).
36. Janardhan, K. S. et al. Toll like receptor-4 expression in lipopolysaccharide induced lung inflammation. *Histol. Histopathol.* **21**, 687–696. https://doi.org/10.14670/hh-21.687 (2006).
37. Moretti, I. F. et al. Late p65 nuclear translocation in glioblastoma cells indicates non-canonical TLR4 signaling and activation of DNA repair genes. *Sci. Rep.* **11**, 1333. https://doi.org/10.1038/s41598-020-79356-1 (2021).
38. Kim, Y. M. et al. Toll-like receptor-2 and −4 in the chorioamniotic membranes in spontaneous labor at term and in preterm parturition that are associated with chorioamnionitis. *Am. J. Obstet. Gynecol.* **191**, 1346–1355. https://doi.org/10.1016/j.ajog.2004.07.009 (2004).
39. Gillaux, C., Méhats, C., Vaiman, D., Cabrol, D. & Breuiller-Fouché, M. Functional screening of TLRs in human amniotic epithelial cells. *J. Immunol.* **187**, 2766–2774. https://doi.org/10.4049/jimmunol.1100217 (2011).
40. Takeuchi, O. et al. Differential roles of TLR2 and TLR4 in recognition of gram-negative and gram-positive bacterial cell wall components. *Immunity* **11**, 443–451. https://doi.org/10.1016/S1074-7613(00)80119-3 (1999).
41. Bolourani, S., Brenner, M. & Wang, P. The interplay of damps, TLR4, and Proinflammatory cytokines in pulmonary fibrosis. *J. Mol. Med.* **99**, 1373–1384. https://doi.org/10.1007/s00109-021-02113-y (2021).
42. Na, K., Oh, B. C. & Jung, Y. Multifaceted role of CD14 in innate immunity and tissue homeostasis. *Cytokine Growth Factor. Rev.* **74**, 100–107. https://doi.org/10.1016/j.cytogfr.2023.08.008 (2023). https://doi.org/.
43. Adams Waldorf, K. M., Persing, D., Novy, M. J., Sadowsky, D. W. & Gravett, M. G. Pretreatment with toll-like receptor 4 antagonist inhibits lipopolysaccharide-induced preterm uterine contractility, cytokines, and prostaglandins in rhesus monkeys. *Reproductive Sci.* **15**, 121–127. https://doi.org/10.1177/1933719107310992 (2008).
44. Gómez-Chávez, F. et al. NF-κb and its regulators during pregnancy. *Front. Immunol.* **12**, 679106. https://doi.org/10.3389/fimmu.2021.679106 (2021).
45. Hadfield, K. A., McCracken, S. A., Ashton, A. W., Nguyen, T. G. & Morris, J. M. Regulated suppression of NF-κb throughout pregnancy maintains a favourable cytokine environment necessary for pregnancy success. *J. Reprod. Immunol.* **89**, 1–9. https://doi.org/10.1016/j.jri.2010.11.008 (2011).
46. Mendelson, C. R. Minireview: Fetal-maternal hormonal signaling in pregnancy and labor. *Mol. Endocrinol.* **23**, 947–954. https://doi.org/10.1210/me.2009-0016 (2009).
47. Robertson, S. A., Skinner, R. J. & Care, A. S. Essential role for IL-10 in resistance to lipopolysaccharide-induced preterm labor in mice. *J. Immunol.* **177**, 4888–4896. https://doi.org/10.4049/jimmunol.177.7.4888 (2006).
48. Fedorka, C. E. et al. Alterations of Circulating biomarkers during late term pregnancy complications in the horse part I: cytokines. *J. Equine Veterinary Sci.* **99**, 103425. https://doi.org/10.1016/j.jevs.2021.103425 (2021).
49. El-Sheikh Ali, H. et al. Equine placentitis is associated with a downregulation in myometrial progestin signaling. *Biol. Reprod.* **101**, 162–176. https://doi.org/10.1093/biolre/ioz059 (2019).

50. Lim, R., Barker, G. & Lappas, M. A novel role for FOXO3 in human labor: Increased expression in laboring myometrium, and regulation of proinflammatory and prolabor mediators in pregnant human myometrial cells1. *Biol. Reprod.* **88**. https://doi.org/10.1095/biolreprod.113.108126 (2013).
51. Khani, H., Feizi, M. A., Safaralizadeh, R., Mohseni, J. & Haghi, M. Altered expression of the HLA-G and IL10RB genes in placental tissue of women with recurrent pregnancy loss. *Clin. Lab.* **69**. https://doi.org/10.7754/Clin.Lab.2022.220822 (2023).
52. Fedorka, C. E. et al. Interleukin-6 pathobiology in equine placental infection. *Am. J. Reprod. Immunol.* **85**, e13363. https://doi.org/10.1111/aji.13363 (2021). https://doi.org/.
53. Osmers, R. et al. Origin of cervical collagenase during parturition. *Am. J. Obstet. Gynecol.* **166**, 1455–1460. https://doi.org/10.1016/0002-9378(92)91619-L (1992). https://doi.org/https://
54. Shi, Y. B., Li, Q., Damjanovski, S., Amano, T. & Ishizuya-Oka, A. Regulation of apoptosis during development: input from the extracellular matrix (review). *Int. J. Mol. Med.* **2**, 273–355. https://doi.org/10.3892/ijmm.2.3.273 (1998).
55. Negara, K. S., Suwiyoga, K., Arijana, K. & Tunas, K. Role of caspase-3 as risk factors of premature rupture of membranes. *Biomed. Pharmacol. J.* **10**, 2091–2098 (2017).
56. Lanci, A. et al. Morphological study of equine amniotic compartment. *Theriogenology* **177**, 165–171. https://doi.org/10.1016/j.theriogenology.2021.10.019 (2022).
57. Castagnetti, C. et al. Evaluation of lung maturity by amniotic fluid analysis in equine neonate. *Theriogenology* **67**, 1455–1462 (2007).
58. Duck-Chong, C. G. The isolation of lamellar bodies and their membranous content from rat lung, lamb tracheal fluid and human amniotic fluid. *Life Sci.* **22**, 2025-2030. https://doi.org/10.1016/0024-3205(78)90549-0 (1978).
59. Lemke, A. et al. Human amniotic membrane as newly identified source of amniotic fluid pulmonary surfactant. *Sci. Rep.* **7**, 6406. https://doi.org/10.1038/s41598-017-06402-w (2017).
60. Hsu, T. Y. et al. The abundances of LTF and SOD2 in amniotic fluid are potential biomarkers of gestational age and preterm birth. *Sci. Rep.* **13**, 4903. https://doi.org/10.1038/s41598-023-31486-y (2023).
61. Zhao, J., Hu, J., Zhang, R. & Deng, J. CEBPD regulates oxidative stress and inflammatory responses in hypertensive cardiac remodeling. *Shock* **60**, 713–723. https://doi.org/10.1097/shk.0000000000002228 (2023).
62. Hart, S. N., Therneau, T. M., Zhang, Y., Poland, G. A. & Kocher, J. P. Calculating sample size estimates for RNA sequencing data. *J. Comput. Biol.* **20**, 970–978. https://doi.org/10.1089/cmb.2012.0283 (2013).
63. Li, C. I., Su, P. F. & Shyr, Y. Sample size calculation based on exact test for assessing differential expression analysis in RNA-seq data. *BMC Bioinform.* **14**, 357. https://doi.org/10.1186/1471-2105-14-357 (2013).
64. Poplawski, A. & Binder, H. Feasibility of sample size calculation for RNA-seq studies. *Brief. Bioinform.* **19**, 713–720. https://doi.org/10.1093/bib/bbw144 (2017).
65. Schurch, N. et al. (ed, J.) How many biological replicates are needed in an RNA-seq experiment and which differential expression tool should you use? *RNA* **22** 839–851 https://doi.org/10.1261/rna.053959.115 (2016).
66. Seyednasrollah, F., Laiho, A. & Elo, L. L. Comparison of software packages for detecting differential expression in RNA-seq studies. *Brief. Bioinform.* **16**, 59–70. https://doi.org/10.1093/bib/bbt086 (2013).
67. Douglas, R. H. & Ginther, O. J. Development of the equine fetus and placenta. *J Reprod. Fertil. Suppl* **23**, 503–505 (1975).
68. Leary, S. L. et al. *AVMA Guidelines for the Euthanasia of Animals: 2013 Edition* (American Veterinary Medical Association, 2013).
69. Conesa, A. et al. A survey of best practices for RNA-seq data analysis. *Genome Biol.* **17**, 13. https://doi.org/10.1186/s13059-016-0881-8 (2016).
70. El-Sheikh Ali, H. et al. Kinetics of placenta-specific 8 (PLAC8) in equine placenta during pregnancy and placentitis. *Theriogenology* **160**, 81–89. https://doi.org/10.1016/j.theriogenology.2020.10.041 (2021). https://doi.org/https://doi.org/
71. Park, Y. S. et al. Comparison of library construction kits for mRNA sequencing in the illumina platform. *Genes Genom.* **41**, 1233–1240. https://doi.org/10.1007/s13258-019-00853-3 (2019).
72. Wang, Z., Gerstein, M. & Snyder, M. RNA-seq: A revolutionary tool for transcriptomics. *Nat. Rev. Genet.* **10**, 57–63. https://doi.org/10.1038/nrg2484 (2009).
73. Andrews, S. & Fastqc A quality control tool for high throughput sequence data. In *Babraham Bioinformatics. Babraham Institute* (2010). https://www.bioinformatics.babraham.ac.uk/publications.html;
74. Bolger, A. M., Lohse, M. & Usadel, B. Trimmomatic: A flexible trimmer for illumina sequence data. *Bioinformatics* **30**, 2114–2120. https://doi.org/10.1093/bioinformatics/btu170 (2014).
75. Kalbfleisch, T. S. et al. Improved reference genome for the domestic horse increases assembly contiguity and composition. *Commun. Biol.* **1**, 197. https://doi.org/10.1038/s42003-018-0199-z (2018).
76. Kim, D., Paggi, J. M., Park, C., Bennett, C. & Salzberg, S. L. Graph-based genome alignment and genotyping with HISAT2 and HISAT-genotype. *Nat. Biotechnol.* **37**, 907–915. https://doi.org/10.1038/s41587-019-0201-4 (2019).
77. Kovaka, S. et al. Transcriptome assembly from long-read RNA-seq alignments with StringTie2. *Genome Biol.* **20**, 278. https://doi.org/10.1186/s13059-019-1910-1 (2019).
78. Pertea, G. & prepDE (eds). py. *Available from*: (2019). https://github.com/gpertea/stringtie/blob/master/prepDE.py;
79. McCarthy, D. J., Chen, Y. & Smyth, G. K. Differential expression analysis of multifactor RNA-seq experiments with respect to biological variation. *Nucleic Acids Res.* **40**, 4288–4297. https://doi.org/10.1093/nar/gks042 (2012).
80. Scott, M. A. et al. Hematological and gene co-expression network analyses of high-risk beef cattle defines immunological mechanisms and biological complexes involved in bovine respiratory disease and weight gain. *PLoS One.* **17**, e0277033. https://doi.org/10.1371/journal.pone.0277033 (2022).
81. Langfelder, P. & Horvath, S. W. G. C. N. A. An R package for weighted correlation network analysis. *BMC Bioinform.* **9**, 559. https://doi.org/10.1186/1471-2105-9-559 (2008).
82. Langfelder, P. & Horvath, S. Eigengene networks for studying the relationships between co-expression modules. *BMC Syst. Biol.* **1**, 54. https://doi.org/10.1186/1752-0509-1-54 (2007).
83. Horvath, S. *Weighted Network Analysis: Applications in Genomics and Systems Biology* (Springer, 2011).
84. Schuhler, S. et al. Feeding and behavioural effects of central administration of the melanocortin 3/4-R antagonist SHU9119 in obese and lean Siberian hamsters. *Behav. Brain. Res.* **152**, 177–185. https://doi.org/10.1016/s0166-4328(03)00260-2 (2004).
85. Ball, B. A., Scoggin, K. E., Troedsson, M. H. T. & Squires, E. L. Characterization of prostaglandin E2 receptors (EP2, EP4) in the horse oviduct. *Anim. Reprod. Sci.* **142**, 35–41. https://doi.org/10.1016/j.anireprosci.2013.07.009 (2013).


## Acknowledgements

The authors would like to acknowledge the support from Dr. Barry Ball and his research lab at the University of Kentucky Gluck Equine Research Center. This work was supported by the VLCS Faculty Grant Texas A&M University (RGS 23-02).

## Author contributions

SM, HE, and YB designed the research. SM, HE, and YB prepared the manuscript. SM and MS performed data analysis. SM, MT, YB, and MS performed the data interpretation. HE and KS were responsible for sample preparation and immunohistochemistry analysis. CF performed the intracervical bacterial inoculation in the exper-

imental group. HE, CF, KS, MT, and YB collected and processed samples. All authors revised the manuscript.

## Declarations

### Competing interests
The authors declare no competing interests.

### Ethical approval
This study was approved by IACUC protocol number 2014-1341.

### Additional information
**Supplementary Information** The online version contains supplementary material available at https://doi.org/10.1038/s41598-025-16671-5.

**Correspondence** and requests for materials should be addressed to Y.B.

**Reprints and permissions information** is available at www.nature.com/reprints.

**Publisher's note** Springer Nature remains neutral with regard to jurisdictional claims in published maps and institutional affiliations.